

Vertical pellet injection in FTU discharges

E. Giovannozzi¹, S.V. Annibaldi¹, P. Buratti¹, B. Esposito¹,
D. Frigione¹, L. Garzotti², S. Martini², M. Marinucci¹,
D. Marocco¹, C. Mazzotta¹, G. Monari¹, M. Romanelli¹,
P. Smeulders¹, D. Terranova², O. Tudisco¹ and FTU Team

¹ Associazione EURATOM-ENEA sulla Fusione, Centro Ricerche Frascati, c.p. 65, 00044 Frascati, Roma, Italy

² Associazione EURATOM-ENEA-CNR sulla Fusione, Consorzio RFX, Corso Stati Uniti 4, I-35100, Padova, Italy

E-mail: giovannozzi@frascati.enea.it

Received 10 December 2004, accepted for publication 31 March 2005

Published 28 April 2005

Online at stacks.iop.org/NF/45/399

Abstract

Central fuelling and pellet enhanced performance modes have been obtained with pellets injected vertically from the high field side on the FTU tokamak. Four phases have been recognized: ablation of the pellets, drifting plasmoids, MHD modes which take the density to the centre of the discharge and finally an anomalous drift which further increases the density peaking. Pellet ablation data have been compared with values from a pellet ablation and deposition code. Comparison between 0.8 and 1.1 MA discharges at a high magnetic field ($B_T = 7$ T) has been carried out: a higher performance has been obtained with the latter due to the higher target density and the larger inversion radius which would increase the effects of $m = 1$ modes to take the density to the plasma centre.

PACS numbers: 52.30.Cv, 52.35.Vd, 52.35.Py, 52.55.Fa

1. Introduction

Fuelling the central plasma region is a major issue in tokamak experiments. The use of pellet injection is considered one of the main methods for fuelling the central plasma region and obtaining a peaked density profile [1]. Furthermore, an improved confinement mode (pellet enhanced performance (PEP) mode) has been observed in several tokamaks with pellet injection [2–4].

Plasmoids [5, 6] are formed during pellet ablation and take pellet material towards increasing major radius. For this reason high field side (HFS) injection is potentially more effective than low field side (LFS) injection in fuelling the plasma core [7]—in fact, the radial drift of the ablated material could take the density to the plasma centre region even if the pellet has been completely ablated before reaching it. FTU (major radius $R = 0.935$ m, minor radius $a = 0.3$ m, circular cross section, maximum achievable toroidal field $B_t = 8$ T, maximum achievable plasma current $I_p = 1.6$ MA, electron density $n_e \sim 10^{20} \text{ m}^{-3}$, molybdenum toroidal limiter and stainless steel main wall) allows us to study the pellet ablation and the drift of the ablated material at a magnetic field and density comparable with that of a burning plasma device.

FTU has two pellet injection systems: a vertical one which is capable of delivering up to three deuterium pellets (mass, 1.5×10^{20} particles each; speed, $500\text{--}600 \text{ m s}^{-1}$) along a vertical chord displaced 0.14 m ($r/a \sim 0.5$) from the

geometrical axis in the HFS direction [8]; and a horizontal one, placed on the equatorial plane, capable of delivering up to seven deuterium pellets (mass, 1.0×10^{20} particles each; speed, 1200 m s^{-1}) from the LFS (figure 1). Both systems have been used—the horizontal LFS system mainly for repetitive PEP mode studies as the high speed pellets can easily reach the centre of the plasma [4] and the vertical one for pellet ablation experiments, but a PEP mode was also obtained with this system.

Two CO_2 interferometer systems were used to determine the plasma density: a fixed one which is fast enough to follow the pellet deposition with a time resolution of $5 \mu\text{s}$, but only along a few chords, and a scanning one which can obtain a line integrated density profile of the full plasma column every $40 \mu\text{s}$ [9]. The temperature was measured on a fast time scale ($10\text{--}50 \mu\text{s}$) by an electron cyclotron emission (ECE) polychromator. Temperature profiles were also measured using a Michelson interferometer every 5 ms and using a Thomson scattering diagnostic. When a laser pulse was available at the proper time a post-pellet density profile was measured by Thomson scattering.

Experiments with the vertical injection system have been mainly carried out at $B_t = 7.1$ T with $I_p = 0.8$ MA and $I_p = 1.1$ MA. The central electron temperature was between 1.2 and 2 keV and the line averaged density range was between 1×10^{20} and $2.5 \times 10^{20} \text{ m}^{-3}$ (figure 2), and only ohmic heating was used.

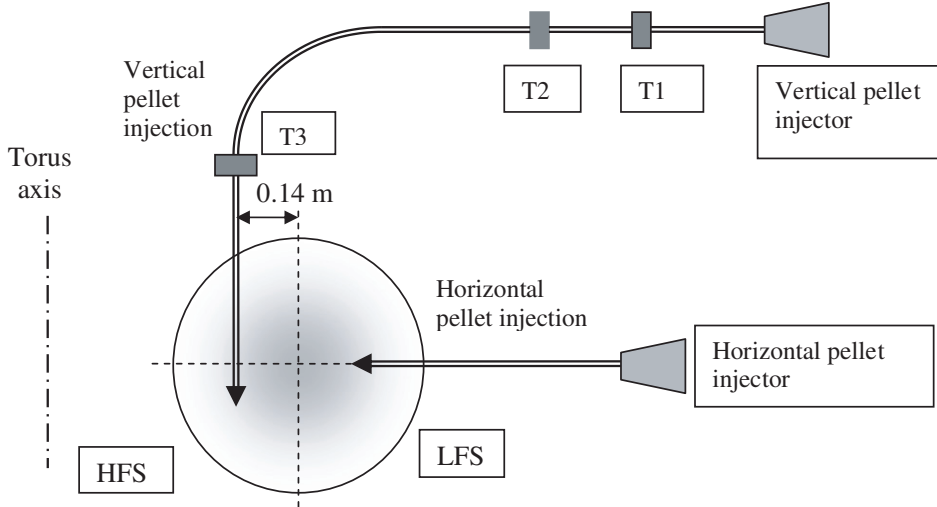


Figure 1. Schematic view of the pellet injection systems installed on FTU (major radius $R = 0.935$, minor radius $a = 0.3$ m). T1, T2, T3 are optical targets which measure the pellet speed. Similar targets are placed on the horizontal pellet injector.

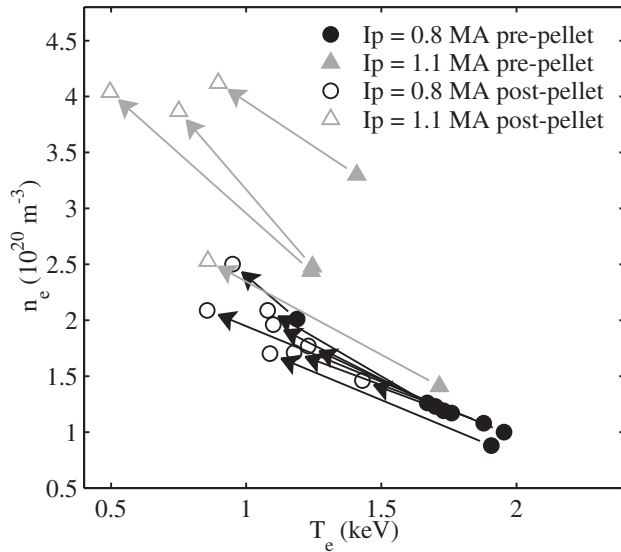


Figure 2. Line integrated density and central temperature in pellet discharges. The full symbols represent pre-pellet values, while the empty symbols are post-pellet values. Black, 0.8 MA discharges; grey, 1.1 MA discharges.

This paper is organized as follows: section 2 describes the pellet ablation and the diagnostics used to follow it, section 3 deals with the following MHD modes, section 4 investigates the performance obtained by vertical injection and makes a comparison with horizontal injection and section 5 gives the conclusion.

2. Pellet ablation

The pellet ablation is diagnosed by H_α emission and Thomson scattering measurements. The H_α light is collected by two optical fibres aligned along the pellet paths (both for the vertical and the horizontal systems). The signals are not absolutely calibrated, and so they are just an indication of the pellet emission. The horizontal optical fibre is basically sensitive

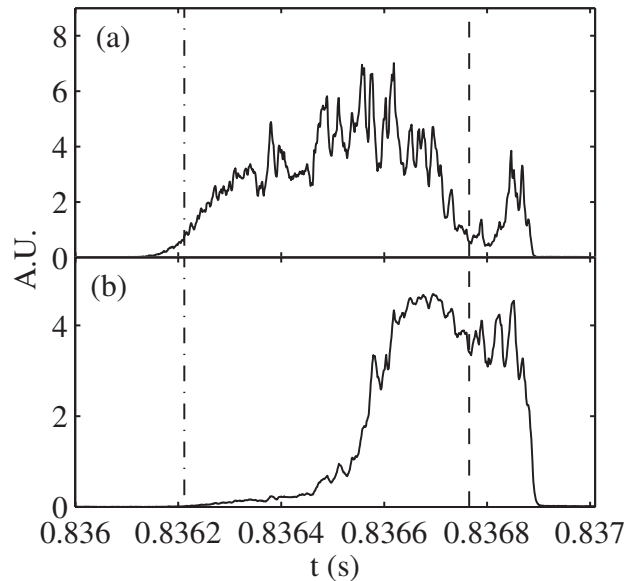


Figure 3. H_α emission in high temperature shot #25254. The dot-dashed line indicates the time when the pellet got into the plasma, while the dashed line indicates the time when the pellet reached the midplane. (a) Signal from the vertical optical fibre. (b) Emission recorded along the horizontal chord.

to light emitted close to the midplane, but at the moment there is no calibration of the acceptance angle.

In almost all discharges with vertical injection the pellet penetrated close to the midplane, and in some cases it went beyond. In figure 3, the H_α signals collected along the vertical and horizontal chords are plotted for discharge #25254 at 1.1 MA. Both signals drop after the pellet has crossed the midplane; the horizontal one is mainly coming from zones close to the midplane as expected. Similar results can be obtained from the rise time of the central chord of the interferometer [10].

In several 0.8 MA discharges Thomson scattering measurements were available less than 1 ms after pellet injection. This was obtained by synchronizing the pellet

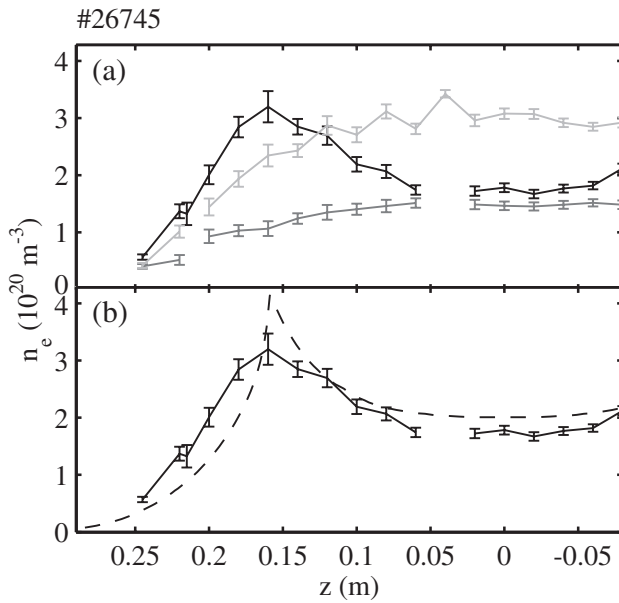


Figure 4. (a) Density profiles as measured from the Thomson scattering in a 0.8 MA discharge: before pellet injection (grey) and 1.2 ms (black) and 35 ms after pellet injection (light grey). The density profile is hollow just after the pellet injection; later the density gets to the plasma centre. (b) Density profile 1.2 ms after pellet injection and a simulation (---) with $v_{\text{plas}} = 500$ m/s and $\lambda_{\text{plas}} = 3.5$ cm.

injection with the Thomson scattering laser pulses. The measured density was hollow initially, while peaked profiles were observed at the next laser pulse, after 33 ms (figure 4).

A simple pellet fuelling calculation was used to simulate the deposited density. The following pellet ablation formula was used:

$$\frac{d(r_p/10^{-3})}{dt} = 1.2882 \times T_e^{1.7153} (n_e/10^{19})^{0.4022} B_t^{-0.0189} \times R^{-0.0940} (r_p/10^{-3})^{-0.5949} C.$$

r_p is the pellet radius, T_e is the electron temperature in kiloelectronvolts and the variable C accounts for small corrections; the full expression can be found in [6].

In effect the density deposition is not very sensitive to the parameters of the ablation formula as the ablation is always close to the midplane due to geometric effects. A point-like plasmoid is assumed to be formed in the simulation every $4 \mu\text{s}$; this plasmoid would drift with a constant velocity v_{plas} and decay exponentially with a decay length λ_{plas} . A grid of magnetic surfaces is used with a Shafranov shift depending on the radius, which approximate the results of equilibrium reconstruction. The plasma density and temperature are assumed to be constant between two consecutive magnetic surfaces, the distance between two of them being about 3 mm. The assumed model for the plasmoids is very crude, but it can give us some useful information by varying v_{plas} and λ_{plas} independently. The plasmoid speed hardly changes the deposition profile for a plasmoid speed larger than the pellet speed and for small λ_{plas} ($\lambda_{\text{plas}} < 0.05$ m). The main effect of the plasmoid speed is to change the zones where pre-cooling of the plasma occurs, reducing the ablation rate—it is mainly a geometric effect due to the vertical injection. On the other hand λ_{plas} strongly affects the deposition zone,

as expected. A simulation is shown in figure 4 for discharge #26745 ($B_t = 7.1$ T, $I_p = 0.8$ MA), and the deposited density is compared with that obtained with the Thomson scattering diagnostic. The simulation has been obtained with a plasmoid speed of 500 m s^{-1} (but plasmoid speeds from 50 up to $50\,000 \text{ m s}^{-1}$ give almost the same results) and $\lambda_{\text{plas}} = 3.5$ cm. The pellet mass has been chosen as $m_p = 1.0 \times 10^{20}$ particles in order to be consistent with the post-pellet volume integrated density. The post-pellet density is reasonably well reproduced by the simulation.

It should be stressed that, in 1.1 MA discharges, a strong $m = 1$ mode gives peaked density profiles in less than 1 ms. This makes synchronization with the Thomson scattering more difficult to realize. In contrast, a hollow density profile could last more than 1 ms in 0.8 MA discharges.

3. MHD modes and central fuelling

Sawtooth oscillations in tokamak discharges are periodic relaxations of the central electron temperature and density which develop when the safety factor on-axis, q_0 , drops below unity. Their temporal traces display a slow rise of temperature in the central region determined by heat deposition and transport, followed by a rapid drop (sawtooth crash) caused by the formation of an $m = 1$ magnetic island, which reconnects field lines in a region between the plasma centre and the mixing radius, which is typically 20–40% larger than the $q = 1$ radius [11]. As explained in [12, 13], horizontal pellets reaching the $q = 1$ surface trigger a reconnection so that the fraction of pellet ablated inside the reconnection region is advected to the plasma centre.

In 1.1 MA discharges with vertical pellet injection a similar behaviour is observed, though a few differences are present: in [12] the pellet was injected along an horizontal chord in the equatorial plane, and the deposition profile was different but the basic phenomenon does not change. The island grows very rapidly, taking the density to the centre in less than 0.5 ms, i.e. the time scale of pellet time of flight. Four phases can be recognized during pellet injection: (1) the pellet is ablated and plasmoids are formed; (2) the drifting plasmoids start affecting the $q = 1$ region; (3) MHD reconnections take the density from the $q = 1$ surface to the plasma centre; (4) a pinch further peaks the density, as shown by Thomson scattering measurements and density profiles obtained inverting interferometer measurements (figure 5).

In the 0.8 MA discharges the situation is different: observations show that the arrival of the pellet does not always trigger the growth of an $m = 1$ magnetic island. The electron temperature evolves across several sawtooth periods, see figure 6.

The density and temperature evolution has been modelled by the MITEV code [11]. The effects of an $m = 1$ magnetic island are accounted for in the code using the characteristic spatial structure of a resistive internal kink mode [14, 15] and the topological constraints of Kadomtsev's model [16]. In [12] the code was used to reproduce density advection by a pellet triggered island. In order to study 0.8 MA discharges the simulation was carried on several sawtooth periods. Each sawtooth advects to the plasma core the fraction of pellet ablated inside the r_{mix} magnetic surfaces (in the theoretical

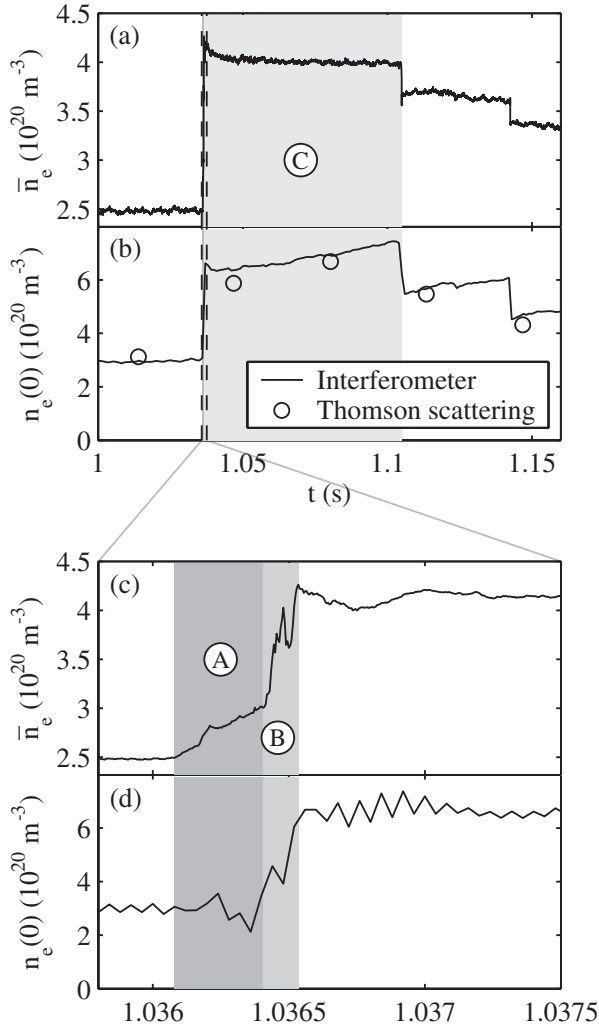


Figure 5. Line average density (a), (c) and central density (b), (d) from interferometer profile reconstruction in high current discharge #25255 ($I_p = 1.1$ MA). Shaded interval A: the pellet is ablated; plasmoids possibly modify the deposition profile (phases 1 and 2). Shaded interval B: a MHD reconnection event takes the density to the plasma centre (phase 3). Shaded interval C: a pinch further peaks the density (phase 4).

model it is assumed that $r_{\text{mix}} = r_{\text{inv}}\sqrt{2}$ and from experimental results $r_{\text{inv}} = 0.08$ m; this model depends on the assumption of an inverse parabolic q profile). Then the density diffusion brings more ablated material inside the r_{mix} surfaces, and this material is advected to the centre in the following sawteeth. But only diffusion was not sufficient to explain the temperature and density profile after a few sawtooth periods. We then added a density pinch of velocity, v_{pi} . The transport equation for density becomes

$$\frac{\partial n_e}{\partial t} = \left\langle \nabla \cdot \left(\left(D_{\perp} \frac{\partial n_e}{\partial \Psi_*} - \frac{n_e v_{\text{pi}}}{|\nabla \Psi_*|} \right) \nabla \Psi_* \right) \right\rangle,$$

where t is the time and Ψ_* is the helical flux function, D_{\perp} is the perpendicular particle diffusivity and v_{pi} is the pinch velocity. The other relevant equations are given in [12].

We run the M1TEV code for discharge #25242. The initial temperature and density are given by the Thomson scattering at $t = 0.835$ s (see figure 7). The perpendicular thermal

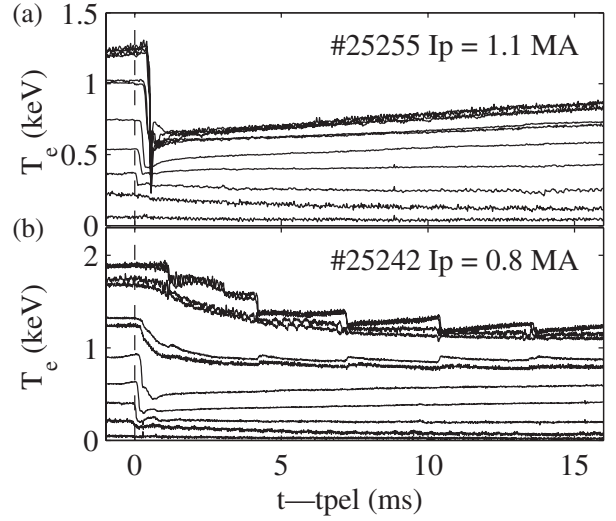


Figure 6. Temporal evolution of electron temperature in two discharges: (a) 1.1 MA discharge, there is a fast reconnection when the pellet gets close to the $q = 1$ surface. This reconnection lowers the central temperature on a very short time scale (0.5 ms). (b) 0.8 MA discharge, reconnection and sawteeth lower the central temperature (and increase the central density) on a longer time scale.

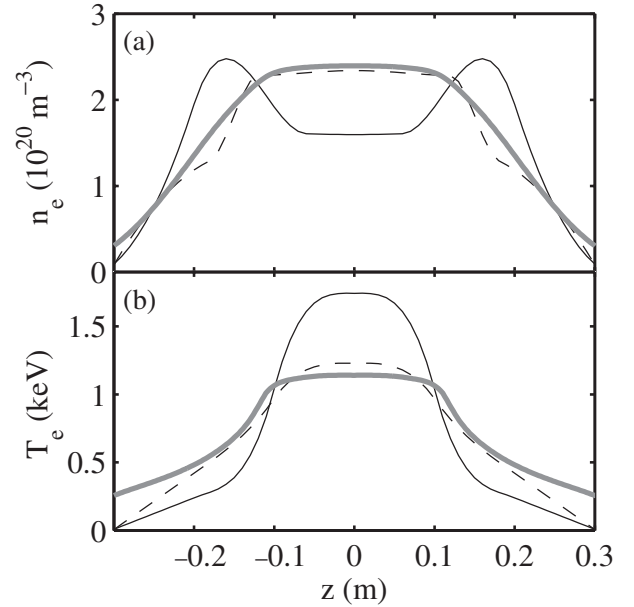


Figure 7. Density (a) and temperature (b) profiles measured by the Thomson scattering are compared with those obtained by the M1TEV code. The pellet is injected at $t = 0.8328$ s. The solid black lines show the post-pellet profiles measured at $t = 0.8345$ s before any reconnection has taken place; these profiles are taken as the initial condition for M1TEV simulation. The dashed lines show the temperature and the density at the following Thomson scattering pulse at $t = 0.8681$ s. The grey lines show profiles at the second Thomson scattering pulse as calculated by the M1TEV code assuming that about six sawtooth reconnections have taken place between the two Thomson scattering pulses.

diffusivity is taken to be of the form

$$\chi_{\perp} = \begin{cases} \chi_{\text{min}} + \chi_{\text{max}} \left(\frac{r_{2\text{sp}}}{a} \right)^2 & r \leq r_{2\text{sp}}, \\ \chi_{\text{min}} + \chi_{\text{max}} \left(\frac{r}{a} \right)^2 & r > r_{2\text{sp}}, \end{cases}$$

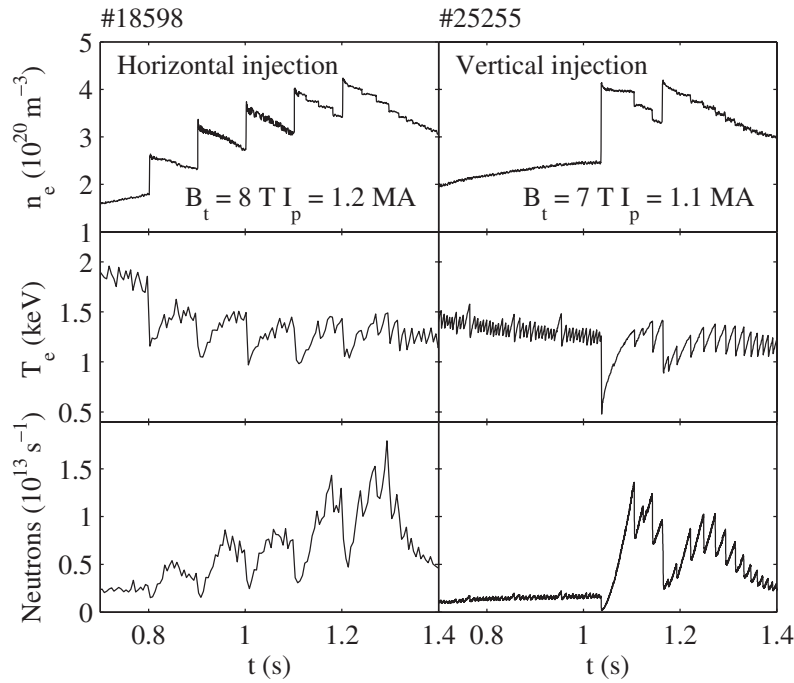


Figure 8. Two discharges with vertical and horizontal pellet injections are compared. They have a similar behaviour, and a PEP mode is obtained in both discharges. The density increase is larger with the vertical pellet injector due to the bigger pellet mass, about 1.5×10^{20} particles, compared with that of the horizontal system (1×10^{20} particles). The target density was also higher than that of the horizontal injection.

where r is the radial coordinate and r_{2sp} is the radius of the island external separatrix, $\chi_{min} = 0.12 \text{ m}^2 \text{ s}^{-1}$ and $\chi_{max} = 1.0 \text{ m}^2 \text{ s}^{-1}$. The perpendicular particle diffusivity is taken constant at $0.17 \text{ m}^2 \text{ s}^{-1}$, and the pinch velocity is

$$v_{pi} = -7.2r \text{ m s}^{-1}.$$

After six sawtooth periods, each one lasting $3 \times 10^{-3} \text{ s}$, we get a reasonable agreement between the experimental and the simulated density and temperature profiles as displayed in figure 7.

Only a small fraction of the density is taken to the centre in 0.8 MA discharges at every sawtooth; the overall density increase and temperature decrease at the centre are slow, lasting a few milliseconds. This is probably due to the smaller inversion radius ($r_{inv}/a = 0.27$) of the 0.8 MA discharges compared with the 1.1 MA discharges ($r_{inv}/a = 0.31$). This kind of analysis does not apply to 1.1 MA discharges where pellet injection triggers a large reconnection. This reconnection takes the density to the centre in less than 0.5 ms, on the time scale of the pellet time of flight (figure 6), and has the same effect as many sawtooth crashes at 0.8 MA.

4. Performance

As mentioned before, after pellet injection there is an increase in the central density and a decrease in the central temperature, but in good discharges where a PEP mode is obtained, on a longer time scale (50 ms typically) the temperature recovers while the density is still high and the density profile is still peaking (figure 8). The overall effect is an increase in the neutron yield and in the confinement time. A line averaged

density of up to $4 \times 10^{20} \text{ m}^{-3}$ has been observed and a neutron yield of 1.4×10^{13} neutrons per second has been obtained. Sometimes, an $m = 2$ mode is triggered after pellet injection, preventing the formation of a subsequent PEP and sometimes leading to a disruption. It has been shown that this is caused by an excessive amount of light impurities (mainly oxygen) in the target plasma. Clean machine conditions permit us to avoid this effect, and multiple PEP modes were obtained with performances similar to those of the multiple PEP modes obtained with the horizontal launcher, as shown in figure 8, in spite of the large distance between the tangential line and the plasma centre. Performances are characterized by a strong reheat of the electrons to the pre-pellet level and a large increase in neutron yield. In this series of experiments, vertical multiple injection was limited to 2–3 successive pellets. Fewer pellets were needed with the vertical injector to achieve the same density and neutron yield of a vertical injected discharge; this was in part due to the larger pellet we had on the vertical system (1.5×10^{20} particles) compared with the horizontal one (1.0×10^{20} particles) and with the higher target density in the discharges fuelled by the vertical system. From our experiments we infer that vertical and horizontal injections have the same efficiency in fuelling the plasma core, but in principle the vertical system could operate at a higher temperature as the plasmoid could help in taking the density close to the $q = 1$ surface.

At 0.8 MA the best performance was obtained in high temperature discharges; in low temperature ones the pellet crossed the midplane without depositing enough particles near the $q = 1$ region. A higher density is favourable in 1.1 MA discharges as the temperature at the ablation zone is always sufficient to have the pellet ablated near the midplane

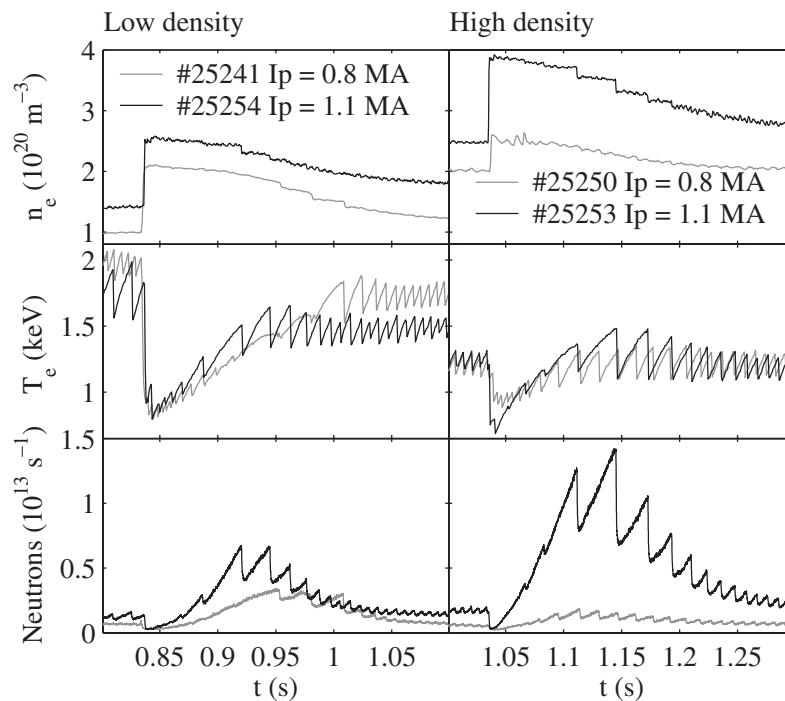


Figure 9. Line integrated density, electron temperature and neutron yield for two low density discharges (0.8 MA, 1.1 MA) and for two high density discharges (0.8 MA, 1.1 MA) during pellet injection. The 1.1 MA discharges have a higher target density than the 0.8 MA ones even at the same temperature. This, associated with the larger inversion radius, gives a better performance, especially at high density.

(figure 9). The larger $q = 1$ radius also helps in having a larger fraction of the pellet particles advected to the plasma centre.

5. Conclusion

Vertical pellet injection has been investigated on FTU. A comparison between vertical and horizontal injections has been carried out. In these HFS injected discharges a synchronized Thomson scattering allowed us to measure the density after pellet ablation.

Four phases have been recognized: pellet ablation, plasmoid drift towards the plasma centre, MHD modes or sawteeth that take the density to the centre and a final density peaking due to a velocity pinch. The MHD central mode triggered by the ablated pellet is a necessary condition for obtaining a good fuelling of the plasma centre. In low current discharges the slower dynamics allowed us to reproduce this mode and the inclusion of a velocity pinch was necessary to find the correct density profile.

The higher current of the 1.1 MA discharges helps the fast reheating of the plasma, and the pre-pellet plasma temperature is restored before the density is lost. A PEP mode has been obtained with a vertical pellet injection in those discharges (1.1 MA) similar to the one already obtained with the horizontal one. In 0.8 MA discharge the fuelling of the centre is not so efficient at a high density, and lower

performances are obtained. On the other hand, high current discharges are more sensitive to oxygen content and can sustain a pellet injection only if they are very clean.

References

- [1] Milora S.L. *et al* 1995 *Nucl. Fusion* **35** 657
- [2] Greenwald M. *et al* 1984 *Phys. Rev. Lett.* **53** 352
- [3] Smeulders P. *et al* 1995 *Nucl. Fusion* **35** 225
- [4] Frigione D. *et al* 2001 *Nucl. Fusion* **41** 1613
- [5] Parks P.B. *et al* 2000 *Phys. Plasmas* **7** 1968
- [6] Garzotti L. *et al* 1997 *Nucl. Fusion* **37** 1167
- [7] Lang P.T. *et al* 1997 *Phys. Rev. Lett.* **79** 1487
- [8] Baker W. *et al* 1995 *Fusion Engineering SOFE '95: 16th IEEE/NPSS Symp. (Champaign-Urbana, IL, USA)* p 1570
- [9] Canton A. *et al* 2001 *Rev. Sci. Instrum.* **72** 1085
- [10] Terranova D. *et al* 2004 *31st EPS Conf. on Plasma Physics (London, 28 June–2 July 2004)* vol 28G (ECA) P-2.101
- [11] Porcelli F., Rossi E., Cima G. and Wootton A. 1999 *Phys. Rev. Lett.* **82** 1458
- [12] Annibaldi S.V. *et al* 2004 *Nucl. Fusion* **44** 12
- [13] Giovannozzi E. *et al* 2004 *Nucl. Fusion* **44** 226–31
- [14] Coppi B. *et al* 1976 *Fiz. Plazmy* **2** 961
Coppi B. *et al* 1976 *Sov. J. Plasma Phys.* **2** 533 (Engl. Transl.)
- [15] Hazeltine R.D. and Meiss J.D. 1992 *Plasma Confinement* (Redwood City, CA: Addison-Wesley)
- [16] Kadomtsev B.B. 1975 *Fiz. Plazmy* **1** 710
Kadomtsev B.B. 1975 *Sov. J. Plasma Phys.* **1** 389 (Engl. Transl.)